Proceedings of IDETC/CIE 2009
ASME 2009 International Design Engineering Technical Conferences &
Computers and Information in Engineering Conference
August 30 - September 2, 2009, San Diego, CA, USA

DETC2009-87657

RIGHT ANGLE TETRAHEDRON CHAIN EXTERNALLY-ACTUATED TESTBED (RATCHET): A SHAPE-CHANGING SYSTEM

Paul J. White*, Chris E. Thorne, Mark Yim

General Robotics, Automation, Sensing, and Perception (GRASP) Lab
University of Pennsylvania
Philadelphia, Pennsylvania 19104
Email: {whitepj, ecthorne, yim}@grasp.upenn.edu

ABSTRACT

Modular robotic systems can form arbitrary shapes that best suit task requirements. Such a system comprised of microscale components could form reconfigurable microstructures or high resolution physical prototypes. This paper presents methods aimed at miniaturization of this programmable matter system towards the millimeter scale or smaller. The Right Angle Tetrahedron Chain Externally-actuated Testbed (RATChET) can be folded into arbitrary 3D shapes. The tetrahedron shaped modules are designed to have limited complexity and employ technologies which can be realized at the microscale. The tools developed to design the module's compliant mechanism can be used to develop small scale modules in the future. Experiments with centimeter scale modules demonstrate that an external actuator can fold a chain of right angle tetrahedrons into 3D shapes. If given the fold pattern to make a shape, a simulator determines the motion sequence for the 2DOF external actuator to fold that pattern.

1 Introduction

Systems that can drastically change their shape can be useful for a variety of applications. If a user needed a specific tool and had a device that could automatically reshape itself into the desired form - a hammer or wrench, for example - the user could replace an entire toolbox with a single device. Similarly, such systems could be made to adaptively conform to a user's hand – a personalized handle for a wrench – or as an interface for a prosthetic. This type of *programmable matter* can form not only one shape, but dynamically change shape multiple times. One of the driving design properties of these systems is the size of the constituting elements - referred to as *modules* in this paper. As the modules become smaller, the feature sizes become smaller (higher resolution) and the number of modules increases (given the same volume). As a result, the number of possible shapes grows, usually exponentially, and things become much more in-

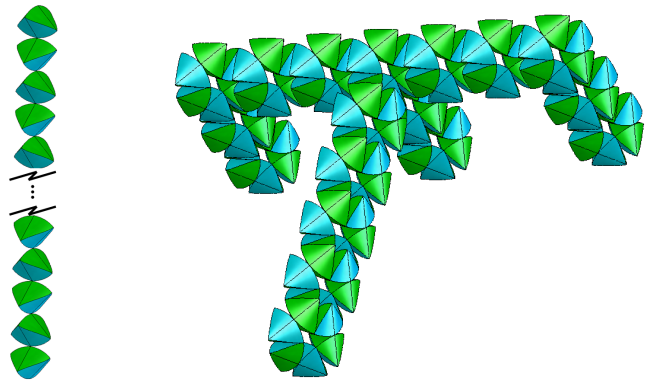

Figure 1: A chain of right angle tetrahedron modules (a) can fold into arbitrary shapes such as a rake (b).

*Address all correspondence to this author.

teresting.

There have been several approaches toward programmable matter including *Modular Self-reconfigurable Robots* and *Self-assembling Structures*. Modular Robots have the flexibility to form a large number of shapes on the fly, but the modules tend to be large. Self-assembling structures can be very small, but they are programmed only once to self-assemble into one shape. The goal of this work is building a reprogrammable shape-changing system that can be miniaturized eventually to the millimeter scale or smaller.

There are numerous implementations of modular robotic systems at the centimeter scale [31]. Modules in lattice style modular robots typically reconfigure by either climbing over neighboring modules [3, 4, 10, 12–14, 24, 29] or by tunelling through the structure [18, 22, 25]. In [32], Yim proposes a rhombic dodecahedron-shaped module that can form arbitrary shapes that are space filling. The mechanisms that move the modules typically make up a majority of the modules' volume, weight, and power consumption, and make miniaturization difficult.

Stochastic modular robotic systems [1, 26, 27] can make modules smaller by eliminating actuators that move the modules. Modules move instead by utilizing external energy that causes the modules to move in a Brownian motion. This motion results in assembly times that are typically slow, with probablistic characteristics. Externally-actuated systems that have deterministic motion [28, 29] do not have internal reconfiguration mechanisms. In this case, the modules are put in an environment that moves in deterministic ways so that inertia will impart forces on the modules in specific patterns, which can then be exploited to cause reconfiguration. While these systems have removed the main actuator and should be easier to miniaturize, they are still on the centimeter scale.

Forming of arbitrary 3D structures at sub-millimeter scales is difficult. Results in the field of self-assembly have demonstrated crystalline structures that are prone to defects and are limited in complexity [8, 30]. MEMS (micro-electro-mechanical systems) techniques such as photolithography have been used to self-assemble structures, but it is inherently a planar technology. Forming 3D shapes requires special techniques such as folding [17]. [5] presents several methods for forming cellular automaton patterns by encoding assembly information in DNA tiles. These are one-time mechanisms that can self-assemble into one shape that is programmed at manufacture time.

In his thesis [6], Griffith proposes adding state information to self-assembly components to achieve arbitrary 3D shapes. He proves a chain of vertex connected squares and a chain of edge connected right angle tetrahedrons can fold into arbitrary 3D shapes. He also demonstrates a chain consisting of four types of square tiles can form desired shapes in the plane. In [6], the information for folding a desired shape is encoded in the order the four types of tiles are placed in the chain. This ordering of types in a given chain hard codes the form of the resulting unique self-assembled shape.

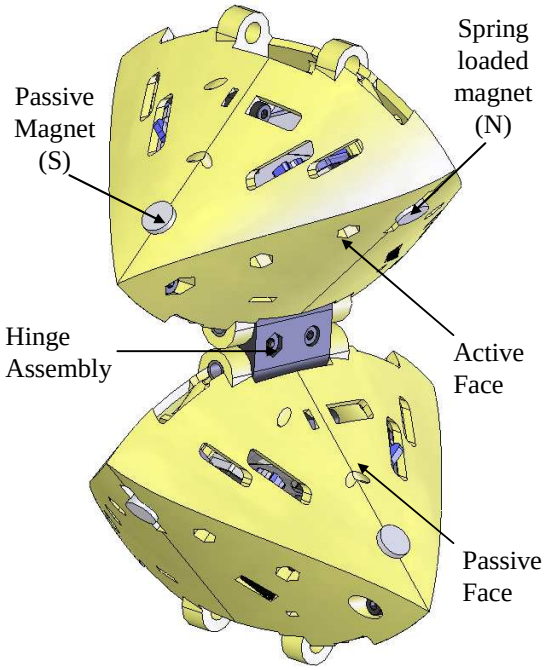

Figure 2: Two RATChET Modules. A module determines which active face will bond with a neigbhor's passive face by releasing a spring loaded magnet.

2 Design

The design of an externally actuated modular robot must adhere to several constraints. One of the goals is to miniaturize the modules; therefore, simplification is an overarching theme. The tradeoff here is often limited functionality. At the centimeter scale, inertial or gravitational forces are used for external actuation. While the main concern of this work is the design of the modules, the size and weight of the modules will also impact the design of the external actuator. The size and number of modules in the final structure is limited by the maximum forces able to be generated by the external actuator.

2.1 Structure and Bonding Mechanism

In order to have a strong close-packed structure, the geometry of the module should be space filling. A cube is one of the simplest space filling polyhedra. However, as stated in [6], a chain of edge connected cubes may not lie flat or straight when unfolded, making the chain difficult to manufacture.

The rhombic dodecahedron has been used as a modular robot [32] as it tiles space. It can also be decomposed into 24 right angle tetrahedrons. Each right angle tetratehedron in the chain is joined to its neighbors by each of its two edges subtended by 90°. This can unfold into a linear chain as shown in Figure 2. The shell of the RATChET module is designed to be lightweight

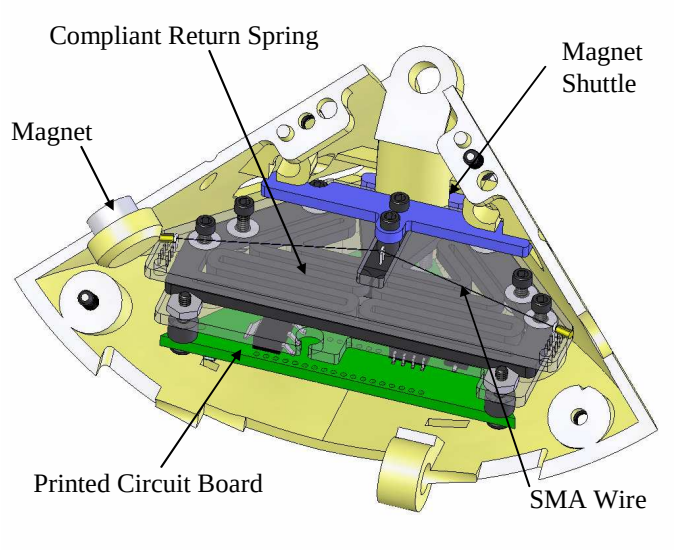

Figure 3: RATChET modules are assembled from two half module subassemblies. Each half contains a Shape Memory Alloy (SMA) actuated magnet release assembly.

and as small as possible while allowing room for the bonding mechanism. The largest dimension of the module is 85mm and a fully assembled module weighs 50g. Adding curvature to the basic tetrahedron eliminates local collision constraints [7].

Modules are joined by a two-axis hinge. Wires for power and communication are routed through the steel tubes of each joint axis, minimizing interference during folding. The hinge assembly shown in Figure 2 is made from two halves that clamp to the steel hinge tubes, which are free to rotate in the hinge mounts on the shell.

Modules bond using Neodymium rare earth magnets. Each module has two passive and two active faces. Each module in the chain is rotated 90° with respect the one before it to allow active faces to bond with passive faces. Figure 2 shows two modules joined by a hinge. The active faces of a module have spring-loaded magnets while the passive faces have a fixed magnet with opposite polarity. Figure 4 shows a cross section view of the bonding mechanism assembly. Before the chain is folded to the desired shape, all spring-loaded magnets are manually retracted (Figure 4a) and held back by a fork shaped latch so that bonding does not occur. This latch is discussed further in Section 2.2. A module can choose to bond in one of two directions. When a module wants to bond on a specific side, it actuates the latch on the active face and releases the magnet (Figure 4b) so that it is capable of bonding. The external actuation manipulator then moves the chain so the module's active face comes in contact with its neighbor's passive face and the magnets bond.

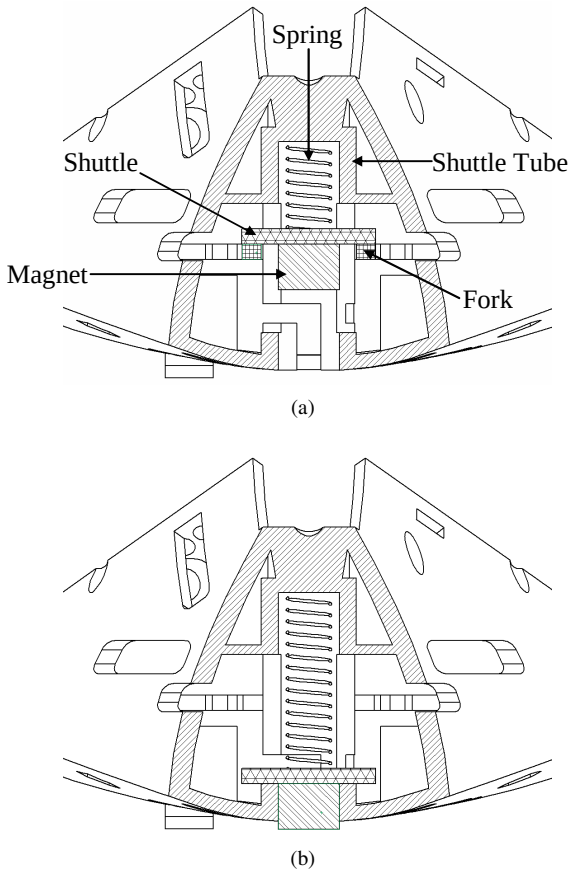

Figure 4: The fork attached to the Compliant Return Spring holds the spring loaded magnet (a). Actuating the SMA retracts the fork and releases the magnet (b).

2.2 Compliant Return Spring Mechanism

The selection of spring-loaded magnetic latching requires the development of a mechanism to release the magnet on command. The mechanism's design and construction should be consistent with the overall vision of this work to explore strategies and design paradigms that are capable of being manufactured at MEMs scale. To this end, the design has features specific to the centimeter scale while adhering to many design principles that apply at smaller scales.

In the case of the RATChET system, effective operation depends on the mechanism's ability to hold and release the magnet. To perform these tasks and to ensure robust operation, the mechanism must provide a method for blocking the shuttle, simplify manual resetting of the latch by the operator, and avoid unintentional release of the magnet due to external disturbances. It should also satisfy several system-wide criteria such as having low weight to allow more modules to be cantilevered during reconfiguration and taking advantage of compliance to accommodate misalignment. Ideally, these mechanisms are replaceable

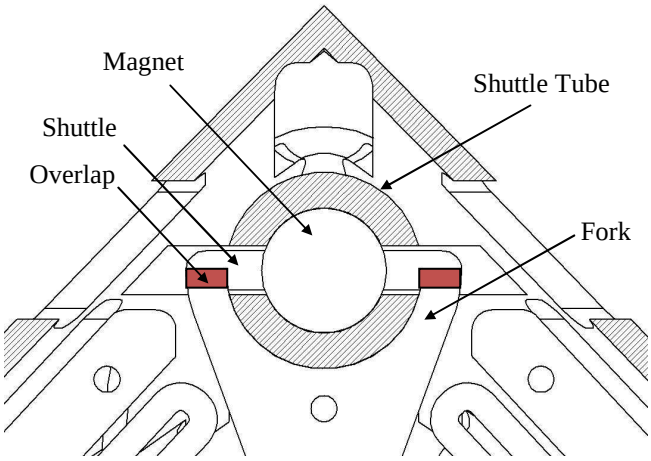

Figure 5: Fork and shuttle cross section.

subassemblies so design modifications are easy to incorporate.

The Compliant Return Spring Mechanism (CRSM) meets the design goals discussed above by being planar, compliant, and manufacturable as a single monolithic part. These attributes facilitate the reproduction of similar designs at smaller scales. The mechanism consists of four layers: the actuation layer, an upper lamina, the compliant return spring layer, and a lower lamina.

A Shape Memory Alloy (SMA) wire actuates a forked end-effector and is fastened to the CRSM assembly with steel staples as shown in Figure 3. Being a solid state actuator, it does not present a barrier to miniaturization. For reliable actuation, the SMA wire requires bias force to return to its unactuated length. The CRSM is designed such that in the unactuated state, the compliant spring provides sufficient bias force.

A serpentine compliant spring design connects the fork to the base of the mechanism and applies the necessary return force required by SMA actuation. The selection of a serpentine spring not only satisfies the tolerance to misalignment goals, but also allows the spring layer to be fabricated from a single planar sheet of material. The SMA wire satisfies more of the design criteria than other actuator technologies considered because it is small, lightweight and easy to replace. The SMA wire's midpoint is attached to the fork, creating a triangle that converts the SMA wire's linear strain of 3% to a 14% deflection of the fork. The necessary increase in deflection is gained at the cost of slightly reduced actuation force. Experiments verify that the actuation force remains adequate to release the shuttle assembly.

The mechanism is assembled to a half-shell as shown in Figure 3. In the nominal configuration, the fork straddles the shuttle tube with its ends blocking the path of the shuttle arms. This is illustrated in Figures 4 and 5 which show a cross section of the tube and fork. When the shuttle is loaded, the coil spring pushes its arms against the underside of the fork, preventing it

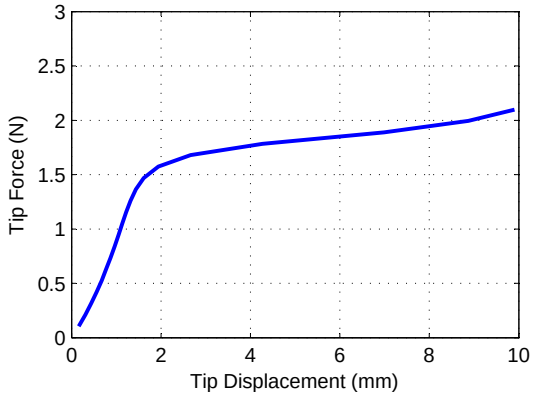

(a)

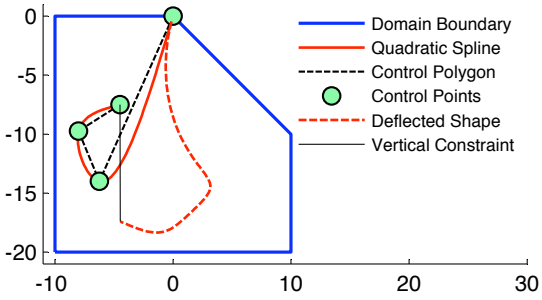

(b)

Figure 6: (a) Force vs. deflection for nonlinear compliant spring. (b) Original and deflected beam.

from traveling to the surface. When the SMA wire is activated, it pulls against the compliant return spring and retracts the fork, releasing the spring-loaded shuttle.

A numerical tool, built in MATLAB, implements a pseudo-rigid-body (PRB) solver and a simple 2D nonlinear finite element-like solver based on the chain algorithm [9]. The latter of the two tools utilizes a graphical interface where B-splines can be manipulated to form arbitrary beam geometries that can be solved to obtain information such as the relationship between force and deflection. These tools allow rapid validation of proposed spring designs and provide an easy way to interface with other built-in and custom MATLAB tools. Promising designs are further analyzed using a standard finite element package. Various constant-force compliant spring designs are being explored with these tools. A constant-force spring will decrease the energy required to activate the SMA wires, thereby allowing for longer chains. Many mechanism configurations and continuous beam geometries such as those proposed by [11], [2] and [20] have been analyzed with this tool and current work includes building an optimizer to solve for various force-deflection profiles of interest. An example of this tool analyzing a constant-force beam is shown in Figure 6. Figure 6a shows the nonlinear force vs.

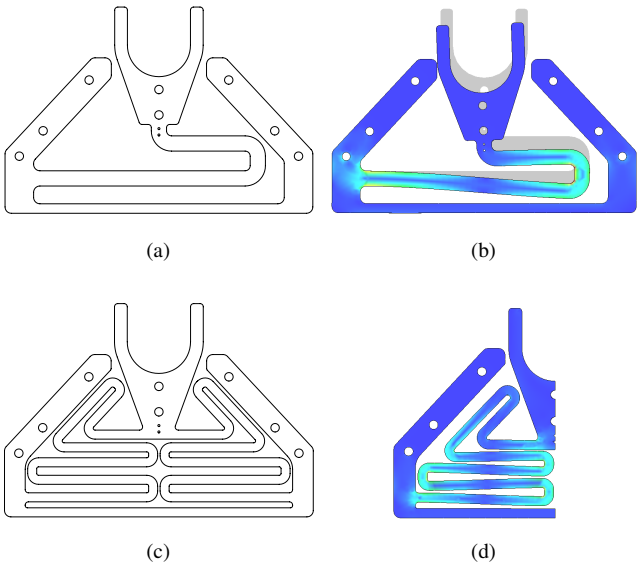

Figure 7: (a) Compliant return spring prototype 1. (b) Compliant return spring prototype 1 finite element results. (c) Compliant return spring prototype 2. (d) Compliant return spring prototype 2 finite element results.

deflection curve for the beam in 6b. The end control point is constrained to move along the vertical constraint.

Several designs for the CRSM were considered and, ultimately, two iterations were prototyped. The second prototype better meets the goals of robustness and scalability of module quantity that the RATChET system demands. To increase robustness, friction within both prototypes is reduced in two key areas: shim washers provide a 0.005 inch gap between the spring and laminae layers and the contact edges between the shuttle and the fork are rounded. The overlap distance between the fork and the shuttle arms directly affects the repeatability of the latching system and is fine tuned through experimentation. To enable scalability in terms of module quantity, the stiffness of the compliant return spring is chosen small enough to minimize the SMA wire activation energy while still providing the necessary return force.

The CRSM is manufactured using a laser cutter because this method satisfies the goals of prototyping large quantities quickly and reliably with planar stock. This choice, however, imposes several constraints on the mechanism's design. Depending on the material, edge quality can suffer during laser cutting due to localized melting near the cutting point. This fact limits the materials that can be used for the compliant return spring to those that provide a minimum repeatable feature size within the scale of interest. Three materials were considered: nylon, acetal and Acrylonitrile butadiene styrene (ABS). All have comparable strength-to-modulus ratios, but, ultimately, ABS produces the best edge quality and allows for a minimum feature size of 0.7 mm.

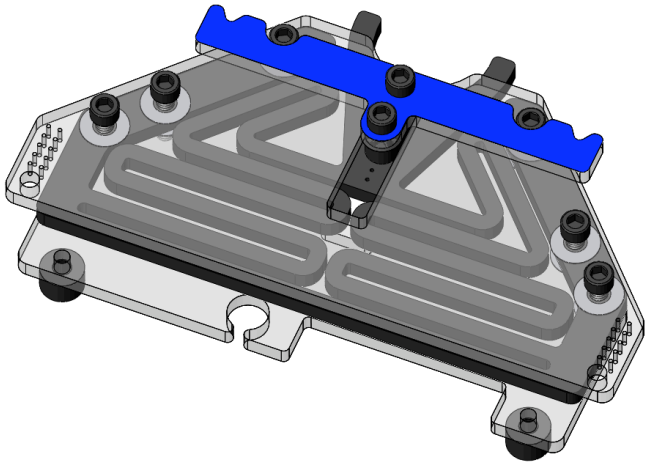

Figure 8: CRSM full assembly.

2.3 Prototype 1

The first prototype meets the majority of the criteria discussed above while minimizing complexity. It consists of a simple serpentine spring that is cantilevered from one side of the base. The other end of the spring forms the fork and is free to move in the plane of the mechanism. The design is shown in Figure 7a. The total displacement of the fork is approximately 3 mm. This configuration creates a nearly linear spring with a constant that can be tuned by modifying the two beam lengths and thicknesses. This design was evaluated in a module and demonstrates a lack of robustness by inconsistently releasing the magnets during actuation. The inconsistency stems from the slight rotation imparted to the fork caused by the asymmetry of the serpentine spring. Figure 7b shows the small rotation of the fork when the spring is deflected.

2.4 Prototype 2

At the expense of design complexity, the second prototype eliminates the fork rotation by using two symmetric serpentine springs which are shown in Figure 7c. This proves to be a much more challenging design problem. Each of the two springs must have a length less than half the width of the mechanism and keep the stiffness low without violating the minimum manufacturable feature size. Unlike the first prototype, the maximum stress plays an important role in designing this double serpentine geometry. Since the length is roughly cut in half, the thickness of the beam needs to be reduced by a factor of 4 to keep the maximum stress the same. This degree of thickness reduction is prohibited by the minimum feature size dictated by the manufacturing process. The required displacement, therefore, must be distributed by filling the available space. The displaced shape of the spring is shown in Figure 7d. The full CRSM assembly can be seen in Figure 8.

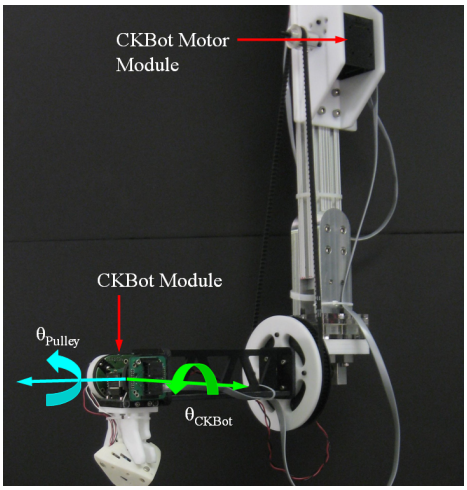

Figure 9: The external actuation system consists of a CKBot module and a CKBot motor module. In the depicted configuration, $\theta_{Pulley} = 0^\circ$ and $\theta_{CKBot} = 0^\circ$.

2.5 Electrical

The electrical subsystem has few basic requirements: onboard processing, inter-module communication, and latch actuation. Each module uses a dsPIC30F4011 microprocessor to run the folding instruction set. Each module has a unique ID and communicates via a CAN bus. The SMA wire is controlled by a 2kHz PWM signal sent to the gate of a FET. The SMA requires 80mA on average to actuate in roughly 2-3 seconds. Relatively slow actuation and under 3-4% strain of the wire ensure the SMA can undergo greater than thousands of cycles.

A six wire bus connects each module with seperate power buses for logic and SMA actuation and the two line CAN bus. These wires are routed between modules through the steel tubes of the hinge assembly. Seperate power buses are essential due to the noise produced when the SMA is actuated. The power buses are connected at a filter block attached to the bracket that mounts the root module to the external actuation system. A $1000\mu F$ capacitor mitigates voltage spikes at the PWM frequency.

3 External Actuation

3.1 System

The external actuation system uses gravity to fold the chain to the desired shape. Gravity forces were chosen over inertial forces as used in [28, 29] to simplify the motion planning and to limit unnecessary collisions. The external actuation system consists of a CKBot module and a CKBot motor module [16, 19] shown in Figure 9. The root module is attached rigidly to the CKbot and they rotate together between 0 and -180°. The CKBot module is mounted via an extension truss to a pulley that is driven by the CKBot motor module to positions between -180° and 180°. In Figure 9, θ_{Pulley} and θ_{CKBot} are both at 0°.

The external actuation system must be strong enough to manipulate a reasonably large number of RATChET modules. Additionally, the joint limits for the external actuators must allow for all types of folds. Section 3.2 discusses the CKBot joint space planning problem and shows the system in Figure 9 can achieve all possible folds.

3.2 External Actuator Motion Planning

Given a desired shape, a folding planner determines the fold sequence which assigns each module one of its two active faces to bond with passive face of its neighbor. Several planners exist which solve the configuration planning problem for modular robotic systems [15, 18, 21, 23]. This section presents an *external actuation motion planner* which given a fold sequence, finds the trajectory for the external manipulator to fold the chain.

To form a desired shape, the CKBot modules move the root RATChET module such that the rest of the chain of modules move under gravity so that desired module joint folds. To simplify the planning, the CKBot and the CKBot motor module move one at a time in 90° increments. Shapes are formed by sequentially folding each module beginning at the root in one of two directions. In order to fold module $i+1$ it is necessary to move module i in a specific path. This equates to finding a path for the root module since modules which have folded (i.e. 1 to i) form a rigid body with the root.

A mapping of the 2DOF of the external actuation is shown in Figure 10. The *CKBot* axis only shows 0 to -180 due the CKBot's joint limits. The *Pulley* axis shows -180 to $+180$ inclusive. Even though -180 and $+180$ are identical positions, the joint limits are reached and so those points are significant to the path planning. With the 90° increments, there are thus 3×5 positions in Figure 10 and so 15 possible positions in the joint space.

Combining this with the two possible orientations of module i and two possible fold directions there are 60 cases to examine. The two general types of orientations for module i correspond to whether the hinge axis between i and $i+1$ is parallel or normal to the CKBot pulley axis. Many of these cases have similar joint space trajectories due to symmetry. Finding a path for all possible initial conditions proves by construction that the external actuation system has sufficient range of motion to achieve any fold type.

Algorithm 1 outlines the fold planning approach. The goal is to find the shortest path in joint space that puts the module to bond, $i+1$, in the proper orientation with respect to module i while adhering to constraints. For a given initial joint position $\Theta_0 = (\theta_{Pulley_0}, \theta_{CKBot_0})$, the algorithm first finds all paths of depth D in the discrete joint space. A single path may visit a joint position more than once since the RATChET modules may change state between visits. It then determines if moving the CKBots along the path (1) adheres to artificial and physical constraints and (2) bonds module $i+1$ to module i. It returns the path if it satisfies these conditions and otherwise increments the

Algorithm 1 Fold Planning

```
Given Θ0 = (θ_Pulley0, θ_CKBot0)
D = 2
loop
    Find all paths of depth D from Θ0
    for each path π_i do
        path_good = TRUE
        for each edge (Θ_k, Θ_{k+1}) in π_i do
            if !is_transition_valid(Θ_k, Θ_{k+1}) then
                path_good = FALSE
                break
            end if
        end for
        if path_good and is_bonded() then
            return π_i
        end if
    end for
    D++
end loop
```

search depth and continues. In this way, the algorithm finds the fewest number of CKBot and pulley 90° rotations to bond module $i+1$ to i.

Constraints are enforced by checking if a transition from one state to the next violates certain rules:

1. *Joint Limits*: $-180^\circ \leq \theta_{Pulley} \leq 180^\circ$ and $-180^\circ \leq \theta_{CKBot} \leq 0^\circ$
2. *Joint Control*: One CKBot moves at a time $\pm 90^\circ$.
3. *Collision Free*: Transitions are invalid if they require a module to pass through another.
4. *Determined*: Transitions are invalid if the position of module $i+1$ is undetermined because it moves to an unstable position (i.e. an inverted pendulum.)
5. *Final Orientation*: The orientation of module $i+1$ at the end of the path must be such that its hinge to module $i+2$ is normal to gravity.

The `is_transition_valid` function in Algorithm 1 returns *FALSE* if moving from Θ_k to Θ_{k+1} violates one of the above rules. Module $i+1$ needs to be a certain orientation with respect to module i to bond. The `is_bonded` function returns *TRUE* if the orientation of module $i+1$ with respect to i is such that active face of i contacts the passive face of $i+1$. The fold direction specifies which active face of i should deploy its magnet to allow a bond to be created with $i+1$.

A kinematic motion planning simulator written in MATLAB verifies the existence of motion paths for all possible fold types. Figure 10 gives examples of valid paths for two sets of initial joint positions. For each case, there are two possible orientations for module i due to the *Final Orientation* rule and two possible fold directions. In Figure 10a, the paths for the last three orientation/fold direction combinations is simply a 90° rotation of one of the CKBot modules. The first case however requires a -90° rotation of the CKBot. Because θ_{CKBot} begins at its negative joint limit, the algorithm needs to find a valid path within the workspace. Note the valid path revisits the $(-180^\circ, -90^\circ)$ position to complete the fold. Likewise in Figure 10b, the 90° orientation, -1 direction case requires a relatively complex path.

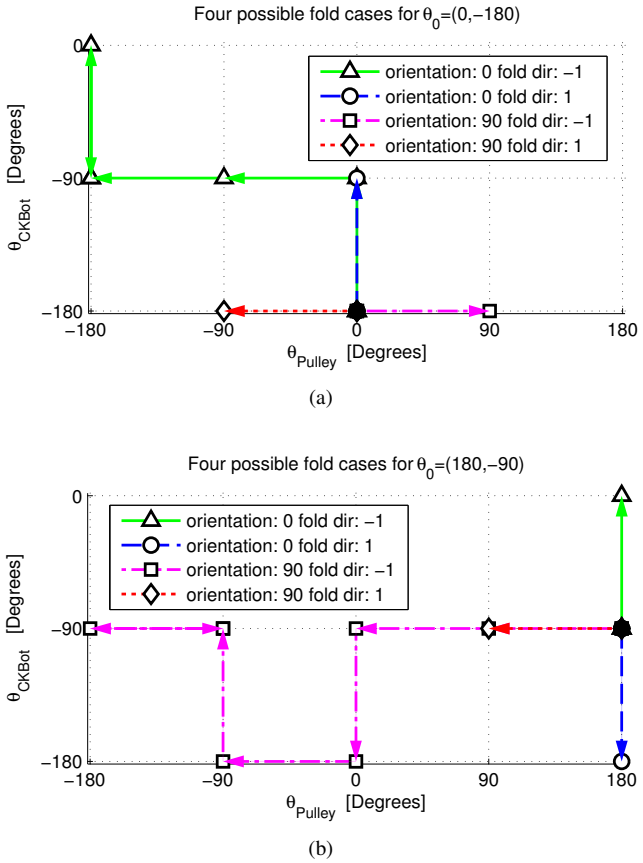

Figure 10: This figure depicts the paths in CKBot joint space for the four possible cases for initial condition (a) $\theta_{Pulley} = 0^\circ, \theta_{CKBot} = -180^\circ$ and (b) $\theta_{Pulley} = 180^\circ, \theta_{CKBot} = -90^\circ$

4 Demonstration

To demonstrate the validity of using external actuation to fold the RATChET system, several demonstrations with five modules were performed. In each demonstration, the root RATChET module coordinates the fold sequence. Using the CAN bus, the root module commands a specific module to bond to the one below it by actuating one of its two bonding mechanisms. This centralized approach limits the amount of information transmitted to and stored on non-root modules. When a module receives the command to bond, it actuates its SMA to retract the CRSM and release the recessed magnet. The ex-

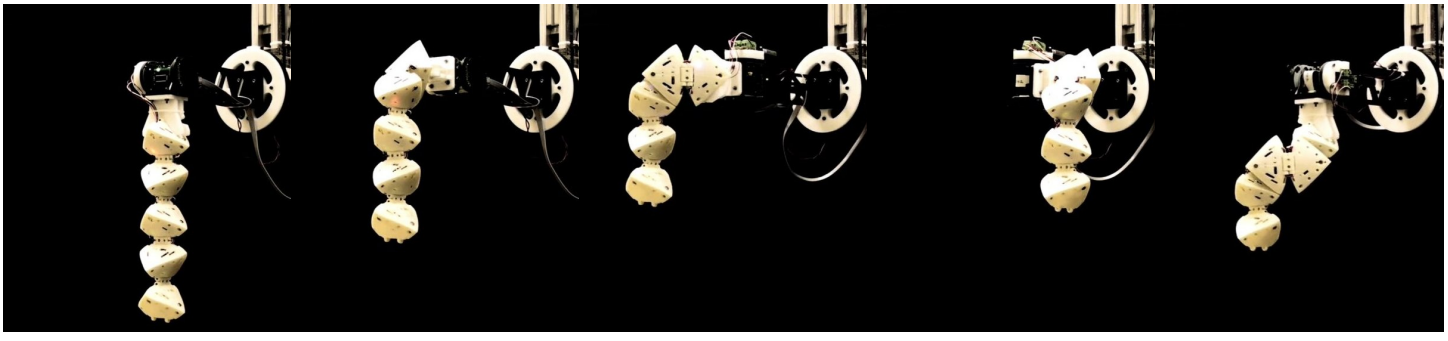

(a) (b) (c) (d) (e)

(f) (g) (h) (i) (j)

Figure 11: Line folding sequence. A chain of five modules (a) folds to a line (j).

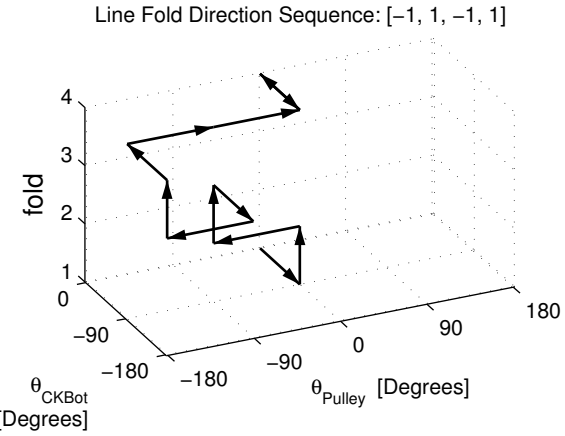

Figure 12: External actuation motion plan for forming a line.

ternal actuation manipulator executes a predifined motion path sychronized with the magnet release of each bonding RATChET module. Both demonstrations form the desired shape in under a minute.

Figure 11 depicts the motion sequence for folding a line from a chain of five modules. Each frame in Figures 11b to 11j shows a change of $\pm 90^\circ$ in either θ_{Pulley} or θ_{CKBot} from the previous frame. Figure 12 shows the motion plan. Each fold level i corresponds to the joint space path to allow module i to bond to $i+1$; vertical arrows indicate transition in the fold sequence. In Figures 11a to 11c, a simple 90° rotation about one of the CKBot joint axes is required to bond a module to its neighbor. Note that the hinge to be folded in Figure 11c is normal to both CKBot axes. It is positioned so that the hinge axis is parallel to the pulley axis (11d) and then bonded (11e).

Figures 11e to 11j show the motion path to bond the final module. Figure 11f illustrates the importance of having a selectable bonding mechanism. If the modules simply had magnetic faces that could not be switched, the last module in the chain would be stuck in the configuration shown in 11f. It is possible that as θ_{Pulley} moved 90° from Figure 11g to 11h that the fifth module would remain above the fourth. To ensure the fifth module bonds to the correct face, the planner moves θ_{CKBot} 90° down (Figure 11i) and then -90° up (Figure 11j). This is indicated by the double headed arrow in the fourth fold in Figure 12.

Figure 13 shows the motion sequence for folding a partial hexahedron (with 5 of the 6 right angle tetrahedrons which make up a hexadron) from a chain of five modules and Figure 14 shows the motion plan. The complexity of the CKBot motion sequence for each fold follows a similar pattern as in the line demonstration. The first fold requires θ_{CKBot} to reach 90° which is beyond

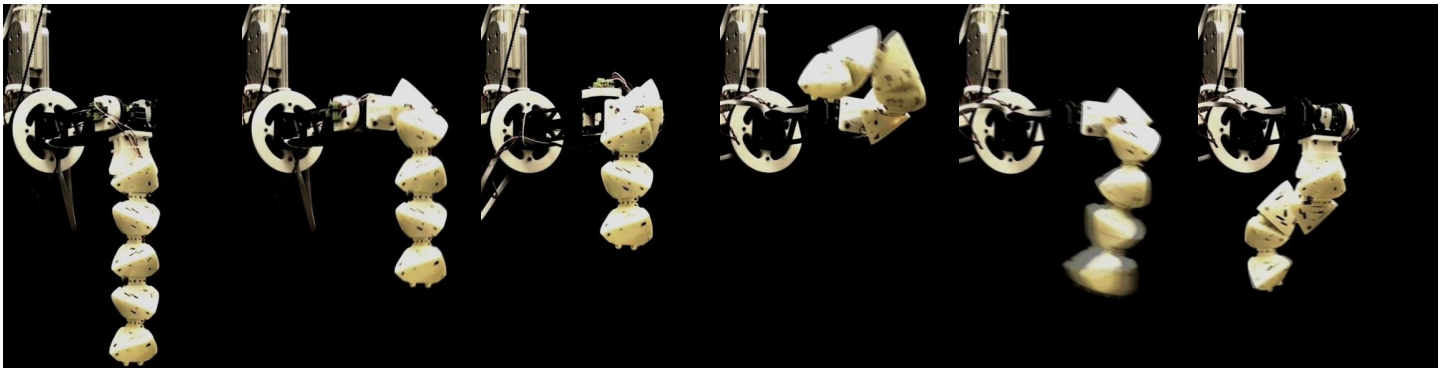

(a) (b) (c) (d) (e) (f)

(g) (h) (i) (j) (k) (l)

Figure 13: Hexahedron folding sequence. A chain of five modules (a) folds to a partial hexahedron (l).

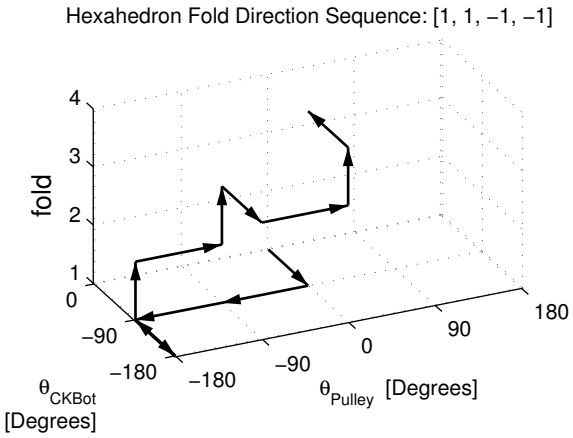

Figure 14: External actuation motion plan for forming a hexahedron.

its joint limits. Initially, θ_{Pulley} cannot move $\pm 90^\circ$ because the second module would move to an unstable position. The valid path first moves θ_{CKBot} to -90° (Figures 13a to 13b). Then θ_{Pulley} moves -180° causing the chain to swing dynamically down completing the first fold (Figures 13b to 13e).

5 Conclusion

The module design is simple and robust. The centimeter-scale latching system is designed for scalability: the mechanism uses planar fabrication technology, monolithic compliant mechanisms, solid-state actuation. The same design approach can be used when creating a RATChET system at the millimeter or even MEMs scales. The compliant return spring mechanism reliably leverages small displacement from SMA wires to large displacement of the recessed magnetic bond. Future work includes developing a switchable latching mechanism that can be retracted to allow modules to break bonds in order to self-reconfigure.

Demonstrations verify that external actuation can be used to manipulate a chain of modules into 3D shapes. Experiments show that using gravity as the external actuation method is reliable and deterministic. A motion planning simulator verifies a 2DOF external actuation system moving in 90° incremements has sufficient range of motion to achieve all types of folds. In addition, the next physical implementation will include sub-centimeter scale modules.

A chain of modules can be formed using gravity forces for

external actuation. At smaller scales where surface forces dominate gravity and inertial forces other external actuation methods will be required such as electric, magnetic, or fluid flow field.

6 Acknowledgements

This work is funded in part by the DARPA DSO Programmable Matter program (PM: Mitchell Zakin.) The authors thank Victor Zykov for a conceptual model of the right angle tetrahedron chain that was extremely helpful for gaining intuition about the system.

REFERENCES

[1] J. Bishop, S. Burden, E. Klavins, R. Kreisberg, W. Malone, N. Napp, and T. Nguyen. Programmable parts: a demonstration of the grammatical approach to self-organization. In *Proceedings of IEEE/RSJ International Conference on Intelligent Robots and Systems*, pages 3684–3691, Edmonton, 2005.

[2] C. Boyle, L.L. Howell, S.P. Magleby, and M.S. Evans. Dynamic modeling of compliant constant-force compression mechanisms. *Mechanism and machine theory*, 38(12):1469–1487, 2003.

[3] J. Campbell, P. Pillai, and S. C. Goldstein. The robot is the tether: active, adaptive power routing modular robots with unary inter-robot connectors. In *Proceedings of IEEE/RSJ International Conference on Intelligent Robots and Systems*, page 4108, Edmonton, 2005.

[4] G.S. Chirikjian. Kinematics of a metamorphic robotic system. In *Proceedings of IEEE/RSJ International Conference on Robotics and Automation*, pages 449–455 vol.1, May 1994.

[5] K. Fujibayashi, R. Hariadi, S.H. Park, E. Winfree, and S. Murata. Toward reliable algorithmic self-assembly of DNA tiles: a fixed-width cellular automaton pattern. *Nano Lett*, 8(7):1791–1797, 2008.

[6] S. Griffith. *Growing Machines*. PhD thesis, Massachusetts Institute of Technology, 2004.

[7] S. Griffith, J. McBride, B. Su, B. Ren, and J. M. Jacobson. Folding any 3D shape. pre published.

[8] K. Hosokawa, I. Shimoyama, and H. Miura. Two-dimensional micro-self-assembly using the surface tension of water. *Micro Electro Mechanical Systems, 1996, MEMS '96, Proceedings. 'An Investigation of Micro Structures, Sensors, Actuators, Machines and Systems'. IEEE, The Ninth Annual International Workshop on*, pages 67–72, Feb 1996.

[9] L.L. Howell. *Compliant mechanisms*. Wiley-Interscience, 2001.

[10] M. W. Jorgensen, E. Hallundbaek Ostergaard, and H. H. Lund. Modular ATRON: Modules for a self-reconfigurable robot. In *Proceedings of IEEE/RSJ International Conference on Intelligent Robots and Systems*, volume 2, pages 2068–2073, Sendai, Japan, 2004.

[11] Christine Vehar Jutte. *Generalized Synthesis Methodology of Nonlinear Springs For Prescribed Load-Displacement Functions*. PhD thesis, University of Michigan, 2008.

[12] K. Kotay, D. Rus, M. Vona, and C. McGray. The self-reconfiguring robotic molecule. In *Proceedings of IEEE/RSJ International Conference on Robotics and Automation*, volume 1, pages 424–431, Leuven, Belgium, 1998.

[13] S. Murata, H. Kurokawa, and S. Kokaji. Self-assembling machine. In *Proceedings of IEEE/RSJ IEEE International Conference on Robotics and Automation*, pages 441–448, San Diego, 1994.

[14] S. Murata, H. Kurokawa, E. Yoshida, K. Tomita, and S. Kokaji. A 3-d self-reconfigurable structure. In *Proceedings of IEEE/RSJ IEEE International Conference on Robotics and Automation*, volume 1, pages 432–439 vol.1, Leuven, Belgium, May 1998.

[15] A. Pamecha and G. Chirikjian. Useful metric for modular robot motion planning. In *Proceedings of IEEE/RSJ IEEE International Conference on Robotics and Automation*, volume 1, page 442, Minneapolis, MN, USA, 1996.

[16] M. Park, S. Chitta, and M. Yim. Isomorphic gait execution in homogeneous modular robots. In *Robitcs: Science and Systems Workshop on Self-reconfigurable Modular Robots, Philadelphia*, 2006.

[17] K.S.J. Pister, MW Judy, SR Burgett, and R.S. Fearing. Microfabricated hinges. *SPIE MILESTONE SERIES MS*, 153:46–53, 1999.

[18] D. Rus and M. Vona. Self-reconfiguration planning with compressible unit modules. In *Proceedings of IEEE/RSJ IEEE International Conference on Robotics and Automation*, volume 4, pages 2513–2520, Detroit, 1999.

[19] J. Sastra, S. Chitta, and M. Yim. Dynamic rolling for a modular loop robot. *Intl. J. of Robotics Research*, 2007.

[20] A. Saxena and GK Ananthasuresh. Topology synthesis of compliant mechanisms for nonlinear force-deflection and curved path specifications. *Journal of Mechanical Design*, 123:33, 2001.

[21] K. Stoy. Using cellular automata and gradients to control self-reconfiguration. *Robotics and Autonomous Systems*, 54(2):135, 2006.

[22] J. W. Suh, S. B. Homans, and M. Yim. Telecubes: mechanical design of a module for self-reconfigurable robotics. In *Proceedings of IEEE/RSJ IEEE International Conference on Robotics and Automation*, volume 4, pages 4095–4101, Washington, DC, 2002.

[23] C. Unsal and P. K. Khosla. A multi-layered planner for self-reconfiguration of a uniform group of I-Cube modules. In *Proceedings of IEEE/RSJ International Conference on*

Intelligent Robots and Systems, volume 1, pages 598–605, Maui, 2001.

[24] C. Unsal, H. Kiliccote, and P. Khosla. I(CES)-Cubes: A modular self-reconfigurable bipartite robotic system. In *SPIE Proceedings, Conference on Mobile Robots and Autonomous Systems*. SPIE, September 1999.

[25] S. Vassilvitskii, J. Kubica, E. Rieffel, J. Suh, and M. Yim. On the general reconfiguration problem for expanding cube style modular robots. In *IEEE/RSJ International Conference on Robotics and Automation*, volume 1, pages 801–808 vol.1, 2002.

[26] P. White, V. Zykov, J. Bongard, and H. Lipson. Three dimensional stochastic reconfiguration of modular robots. In *Robotics: Science and Systems*, pages 161–168, Cambridge, 2005.

[27] P. J. White, K. Kopanski, and H. Lipson. Stochastic self-reconfigurable cellular robotics. In *Proceedings of IEEE/RSJ IEEE International Conference on Robotics and Automation*, volume 3, pages 2888–2893, New Orleans, LA, USA, 2004.

[28] P. J. White and M. Yim. Scalable modular self-reconfigurable robots using external actuation. In *Proceedings of IEEE/RSJ International Conference on Intelligent Robots and Systems*, pages 2773–2778, San Diego, 2007.

[29] P. J. White and M. Yim. Reliable external actuation for extending reachable robotic modular self-reconfiguration. In *International Symposium on Experimental Robotics*. IFRR, July 2008.

[30] G.M. Whitesides and M. Boncheva. Supramolecular Chemistry And Self-assembly Special Feature: Beyond molecules: Self-assembly of mesoscopic and macroscopic components. *Proceedings of the National Academy of Sciences of the United States of America*, 99(8):4769, 2002.

[31] M. Yim, W.-M. Shen, B. Salemi, D. Rus, M. Moll, H. Lipson, E. Klavins, and G. S. Chirikjian. Modular self-reconfigurable robot systems [grand challenges of robotics]. *IEEE Robotics and Automation Magazine*, 14(1):43, 2007.

[32] M. Yim, Y. Zhang, J. Lamping, and E. Mao. Distributed control for 3D metamorphosis. *Autonomous Robots*, 10(1):41–56, 2001.